Biochemical and Biophysical Research Communications **264,** 181–185 (1999)
Article ID bbrc.1999.1498, available online at http://www.idealibrary.com on IDEAL®

Multiple Domains of DFF45 Bind Synergistically to DFF40: Roles of Caspase Cleavage and Sequestration of Activator Domain of DFF40

John S. McCarty, Shen Yon Toh, and Peng Li[1]
Laboratory of Apoptosis Regulation, Institute of Molecular and Cell Biology, 30 Medical Drive, Singapore 117609, Singapore

Received September 9, 1999

CAD/DFF40, the nuclease responsible for DNA fragmentation during apoptosis, exists as a heterodimeric complex with DFF45/ICAD. The study presented here augments the accompanying inhibition and chaperone study with an analysis of specific binding strengths and locations of DFF45 binding sites within DFF40. This allows us to show that DFF40/45 interaction is mediated by binding of three functional domains (D1, D2, and D3) of DFF45 to two domains (activator and catalytic) of DFF40. D1 binds exclusively to the activator domain and D2 binds to the catalytic domain of DFF40. Inhibition of DFF40 nuclease activity arises independently from D1 functional sequestration of the activator domain and D2 blockage of the catalytic domain of DFF40. The mechanism of caspase activation of DFF40 is the disruption of the synergistic binding activity of DFF45 domains to DFF40 after caspase recognition and cleavage of DFF45 in the context of a DFF45/40 complex. © 1999 Academic Press

Key Words: **apoptosis; CAD and ICAD; DNA fragmentation; BIAcore; DFF40 and DFF45.**

DNA fragmentation is a basic hallmark of cells undergoing apoptosis (1) and has been shown to be mediated by the action of the DFF40 (CAD) nuclease which is isolated with an inhibitor protein DFF45 (ICAD) (2–7). DFF40 can be activated after caspase 3, a downstream caspase in the apoptosis activation cascade, cleaves at two caspase consensus sites in DFF45. In the accompanying study (8), we investigate the reported chaperone activity of DFF45 (2, 7) and show that one aspect of this activity involves maintaining the solubility of mature DFF40. Furthermore, we found that the N-terminal region of DFF45 is critical to maturation of DFF40, presumably by interaction with nascent DFF40. The most intriguing observation, however, was to show that two separate fragments of DFF45 independently inhibit DFF40 DNAse activity. These two fragments (D1 and D2), corresponding to the two N-terminal fragments of DFF45 generated by caspase cleavage, therefore define functional domains of DFF45. However, though the isolated domains of DFF45 were able to inhibit DFF40 nuclease activity, we were unable to isolate these fragments as expected during co-immunoprecipitation of DFF40 from mammalian cells. This low sensitivity of the immunoprecipitation assay and the existence of endogenous DFF40/45 in the mammalian cells, led us to consider alternative methods to further characterize the DFF40/45 interaction *in vitro.*

The use of the Biacore systems (9, 10) allowed us to quantify the interaction of the two inhibitory domains and the third C-terminal domain of DFF45 with active DFF40. Furthermore, we are able to map the binding of these domains to two separate domains of DFF40. This analysis, coupled with the results in the accompanying paper (8), allow us propose an integrated model on the mechanisms of DFF45 chaperone and inhibition activities and subsequent activation of DFF40 by caspase 3.

MATERIALS AND METHODS

Plasmid construction and protein production and purification. D40(Δ80) and D40(Δ117) fragments were expressed as C-terminal His fusions from similar constructs as those used with DFF45 (8). DFF40, DFF45 and truncated forms of DFF45 (D1, D2, D3, D1-2 and D2-3) were generated and purified as described (8). Fragments of DFF40 were purified from bacteria similar manner as described for DFF45 (8). The fragments were first isolated on Ni^{++} columns and then further purified on a mono S column (Pharmacia).

BIAcore experiments. The experiments were performed on a BIACORE 2000 machine in buffer D containing 100 mM KCl. DFF40 or its fragments were immobilized to CM5 chips at pH 7 using the amine coupling kit according to the manufacturer's directions (BIAcore AB). During kinetic analysis, the analytes were in general

[1] To whom correspondence should be addressed. Fax: 65-779-1117. E-mail: mcblip@imcb.nus.edu.sg.

0006-291X/99 $30.00

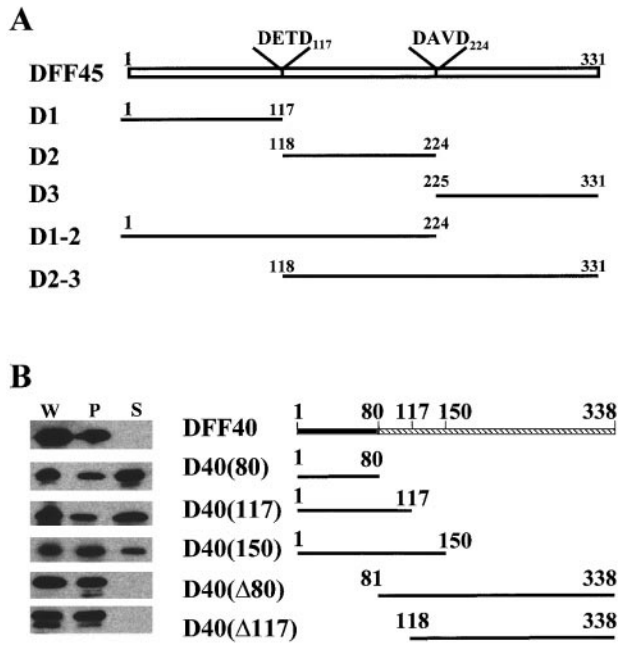

FIG. 1. (A) Fragments of DFF45 and (B) DFF40 used in the Biacore experiments characterizing the interaction of DFF45 with DFF40. The solubility of the DFF40 and its fragments during expression were analyzed by Western blot analysis of whole cell (w) and post-lysis supernatant (s) and pellet (p) fractions with anti-DFF40 antibodies.

injected to the flow cells at a flow rate of 10 μl/min and allowed to bind for 3 minutes before allowing dissociation at the same flow rate. DFF45, D1-2 and D2-3 were present at 10 μM concentration while D1, D2, and D3 were present at 50 μM. Bulk effect and background binding were controlled by subtracting the signal from a flow cell containing either no bound protein or bound GST. For equilibrium analysis, the KD was calculated from the plot of RU(eq)/C versus C after allowing the binding to come to equilibrium at a flow rate of 3 μl/min. Shown in the figures are representational injections from multiple examples.

RESULTS AND DISCUSSION

Monitoring DFF40/45 interactions with the BIAcore system. We purified DFF40, DFF45 and fragments of DFF45 that correspond to the single and double fragments of DFF45 expected after cleavage at the caspase consensus sites in DFF45 (Fig. 1a). For the Biacore experiments, DFF40 was immobilized on the chip surface while DFF45 and its fragments were injected as analytes in the soluble phase. DFF45 binding was clearly observed by the increase in the resonance signal, which dissipated during the subsequent dissociation phase (Fig. 2). In addition, all three isolated fragments of DFF45—D1, D2, and D3—gave rise to increased mass on the chip surface indicating that they each bind to DFF40 directly (Fig. 2). The kinetics of interaction between D1 and DFF40 or D3 and DFF40 were rapid for both association and dissociation. Within the time resolution of the BIAcore machine, only traces of the kinetics were observed in the shallow slope at saturation during the binding phase and in the small tail during the dissociation phase. In contrast to D1 and D3, the binding of D2 to DFF40 demonstrated slower kinetics. However, the kinetics of D2 interaction was qualitatively much different from that of full-length DFF45 interaction with DFF40. In particular, the dissociation of the isolated D2 domain was much more rapid than full-length DFF45. We established the dissociation constants (K_D) of D1, D2 and D3 for DFF40 at 18, 6 and 14 μM, respectively, by examining the extent of equilibrium binding at various ligand concentrations (Inset, Fig. 2). The discreet binding of these fragments reiterates their status as independent, functional domains of DFF45 concluded from the accompanying DFF40 nuclease inhibition study (8).

Consistent with the immunoprecipitation experiments presented in the accompanying report (8), fragments of DFF45 corresponding to double domains D1-2 and D2-3 demonstrated significantly more stable binding to DFF40 than isolated domains. The dissociation phase for the double domain binding is much more extensive than D2, the most stable single domain. The increase in binding strength through inclusion of the third domain was *ca.* 4X, reflected in the K_Ds of 10, 8, and 2 nM for D1-2, D2-3 and full-length DFF45, respectively, obtained by fitting of the observed data to

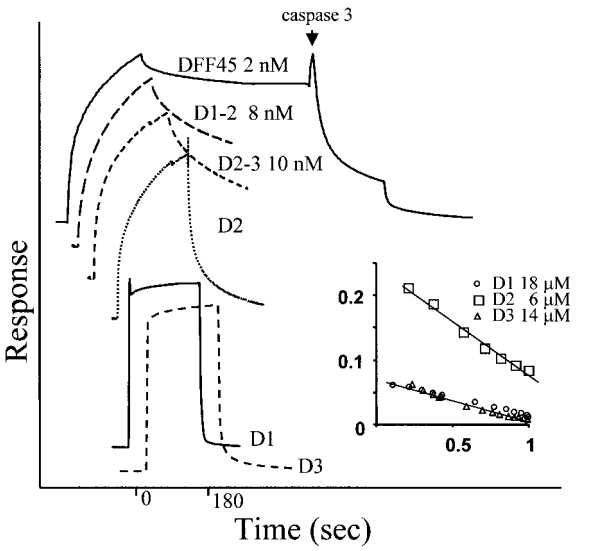

FIG. 2. Interaction of DFF45 and its fragments to immobilized DFF40 was observed by plasmon resonance using a BIAcore machine. Association was allowed to occur for 3 minutes at 10 μl/min followed by a period of dissociation. Curves were normalized to allow clear comparisons of signal loss during the dissociation phase. The arrow above the dissociation phase of DFF45 indicates the time point when purified caspase 3 was injected. The kinetics associated with D1, D2, and D3 were fast enough to allow KD determination based on the extent of binding at various analyte concentrations. Shown in the inset is the plot of relative binding/concentration (μM) as a function of relative binding. K_D for DFF45, D1-2, and D2-3 were calculated from kinetic data assuming bivalent interaction.

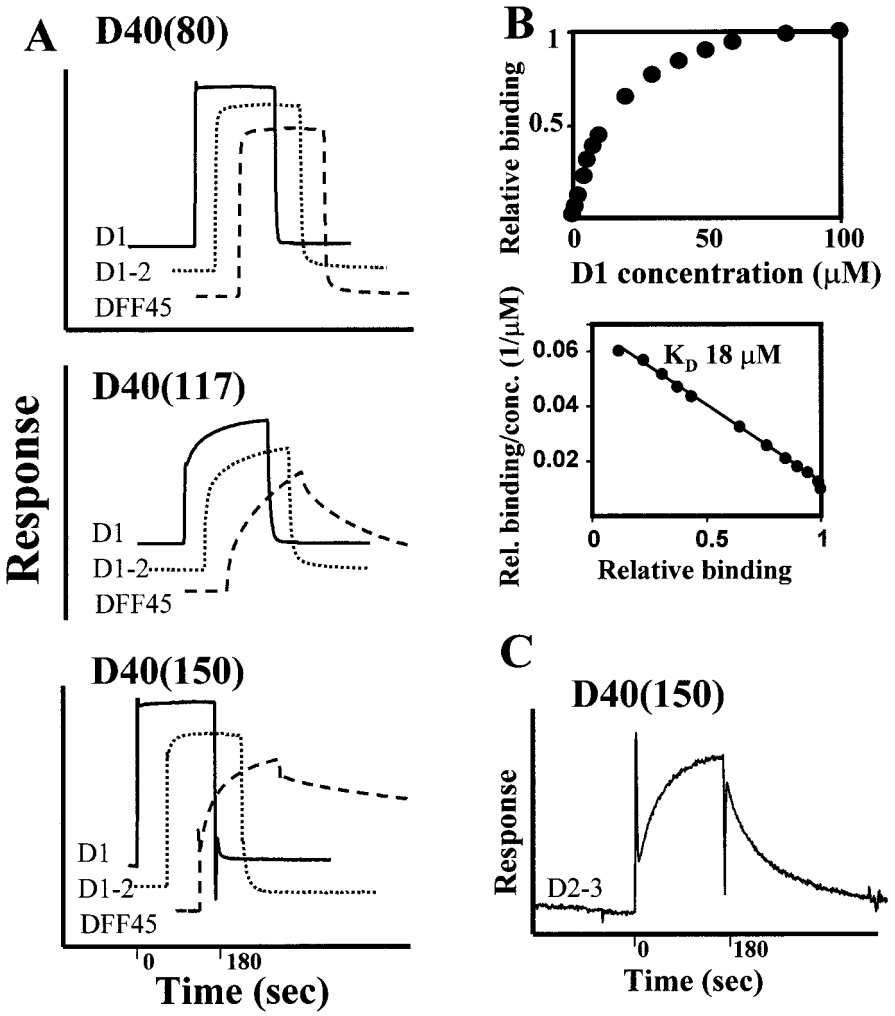

FIG. 3. Interaction between domains of DFF45 and truncated forms of DFF40. (A) N-terminal truncations of DFF40, D40(Δ80), and D40(Δ117) displayed an insolubility during expression in *E. coli* similar to that of full-length DFF40. W, P, and S represent the amount of DFF40 presented in whole cell lysate (W), pellet (P), and supernatant (S) respectively. (B) Purified N-terminal fragments of DFF40 were immobilized on BIAcore chips and analyzed for binding by fragments of DFF45. Curves were normalized to allow clear comparisons of signal. (C) The K_D of DFF45 D1 binding to D40(80) was determined by saturation binding at various concentrations of D1. (D) A weak signal observed for D2-3 binding to D40(150).

binding curves assuming bivalent binding characteristics (data not shown). Caspase 3 injection during the dissociation phase resulted in a large increase in the dissociation rate of bound DFF45—presumably due to cleavage at caspase sites exposed on the DFF40/45 complex. This experiment graphically demonstrates the mechanism of caspase activation of DFF40 is through recognition of sites exposed on the DFF40/45 complex followed by proteolytic cleavage of DFF45, resulting in rapid complex dissociation.

A fundamental finding of our studies is that DFF45 domain architecture consists of three fully independent domains, in terms of their ability to bind to DFF40 as well as repress DFF40 activity. The boundaries of these functional domains (D1, D2 and D3) coincide with the two caspase-cleavage sites. Furthermore, the boundary of D1 also coincides with the extent CIDE-N homology (11) while a putative coil-coil structure motif additionally delineates the C terminal extent of D2 (data not shown). While all three domains bind to DFF40 with relatively low affinity (μM K_D), synergistic binding strength was observed when two domains were covalently linked together (D1-2, D2-3 and full length DFF45, low nM K_D). This synergism appears to arise from the cumulative effect of the individual binding strengths as no evidence of interactions between DFF45 domains was observed. As demonstrated in the accompanying paper (8), repression was found to be fully encoded in individual domains. Taken together, our data clearly indicate a repression mechanism

based on synergistic binding of DFF45 domains to DFF40 and subsequent activation through disruption of the binding synergy by caspase cleavage.

Localization of DFF45 binding sites in DFF40. To better understand the mechanism of DFF45 activities in regard, we constructed several N-terminal and C-terminal truncations of DFF40 and isolated the recombinant proteins for analysis with BIAcore (Fig. 1b). Unfortunately, both N-terminal deletions [D40(Δ80) and D40(Δ117)] could not be expressed as soluble protein (Fig. 1b). In contrast, all three C-terminal truncations D40(80), D40(117) and D40(150) were found to be either predominantly soluble or, in the case of D40(150), partially soluble. Considered together, these observations localize the elements in DFF40 inferring the insolubility observed *in vitro* and during expression in *E. coli.* These insoluble elements map distal to residue 117 of DFF40 with the strongest elements mapping distal to residue 150.

The D40(80) fragment of DFF40 was defined by its homology to sequences within D1 of DFF45 and in N-terminal sequences of CIDE-A and CIDE-B (data not shown; 11, 12). BIAcore analysis reveals that these homologous regions fully define the interaction of DFF45 D1 to DFF40 (Fig. 3). D1 binding to D40(80) immobilized on the chip was nearly identical to that with full-length DFF40, with a measured K_D of 16 μM (Fig. 3, panel C). Furthermore, no alteration in binding was observed by the additional domains in D1-2 and full-length DFF45 and no interaction of isolated D2 or D3 with D40(80) was observed by BIAcore (data not shown). In conclusion, D1 binding maps exclusively to D40(80), an homologous, soluble and functional domain of DFF40, while D2 and D3 bind exclusively to more distal elements.

BIAcore analysis with the two additional C-terminal truncations of DFF40, D40(117) and D40(150), allowed refinement of the binding of the remaining DFF45 domains, D2 and D3. While the binding of D1-2 to immobilized D40(117) was similar to that observed with the isolated D1, full-length DFF45 had much more stable binding, indicating that D3 binding maps in part to the region between residues 81 and 117. The stabilization of binding of full-length DFF45 relative to D1-2 was even more enhanced with D40(150) immobilized on the chip. In addition, a very weak signal was observed during injection of double domain D2-3 (Fig. 3, panel D). This signal was qualitatively very different from that observed for isolated D3 binding to DFF40 but similar to that observed for D2 (Fig. 2). This suggests that partial D2 binding may be present in the residues up to 150, probably distal of residue 117, allowing for the additional stabilization of DFF45 binding. However, as neither isolated domain D2 or D3 gave rise to any signal during BIAcore analysis with these

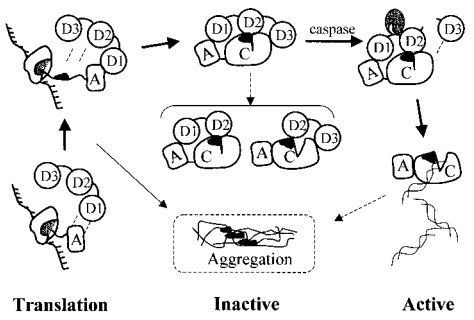

FIG. 4. Mechanism of DFF45 chaperone and repression functions with DFF40 and subsequent activation by caspase. DFF45 (consisting of independent domains D1, D2, and D3) initiates interaction during translation of DFF40 from the ribosome, when the N terminal domain of DFF45 (D1) binds exclusively to a soluble domain (A) containing the first 80 residues of DFF40 with rapid kinetics. This initial binding is critical for expression of soluble DFF40 presumably through stabilization of D2's binding to distal regions of DFF40 inferring insolubility (dark area). The high stability of the DFF40/45 complex guarantees concomitant repression as well as solubility of DFF40. Similar stability is also observed for complexes containing only two adjacent DFF45 domains, which may play roles in alternative DFF40 regulatory pathways. Binding of either D1 or D2 is sufficient to block nuclease activity, suggesting that the N-terminal domain of DFF40 functions to Activate (A) the distal Catalytic domain (C). Inhibition thus occurs independently through sequestration of the Activator domain by D1 or blockage of the catalytic domain by D2. Caspase activation of DFF40 occurs after two interdomain sites of DFF45 in the DFF40/45 complex is recognized and cleaved. Cleavage at the interdomain sites disrupts synergistic binding of DFF45 domains resulting in rapid dissociation of the complex and activation of DFF40 as a nuclease.

C-terminal truncations (data not shown), the residues up to 150 do not fully encode a binding site for either.

Integrated model of the interaction of DFF45 with DFF40. Our discovery that the first 80 residues of DFF40 form a stable and soluble fragment encoding full binding to D1 leads to the consideration of this region as a functional domain or subdomain of DFF40. Such domain assignment is also consistent with the limited homology observed between this region and residues in D1. Exclusive binding of D1 inhibitor domain to this region of DFF40 demonstrates the critical role of this N-terminal domain in DFF40's nuclease activity. The simplest interpretation is that this domain of DFF40 interacts with, and subsequently activates, the distal C-terminal domain. In such a model, the N-terminal domain then functions as an Activator domain and the C-terminal domain thus functions as the Catalytic domain (Fig. 4). D1 functionally sequesters this Activator domain by binding to this region. A related proposal of a regulatory domain encoded by the N-terminal half of DFF40 was made in a recent publication where partial nuclease activity was reported to be associated with C-terminal region of DFF40 (12). Unfortunately, we found C-terminal region of DFF40 to be insoluble during bacterial expression and could not be isolated as an active protein. We note in this

model that an economic mechanism of D2 inactivation is blockage of the active site in the C-terminal domain of DFF40.

One apparent paradox in these two studies is the strict requirement of D1 for maturation of DFF40 *in vivo* (8) despite the mapping of D1 binding region to the first 80 residues, a functional domain of DFF40 that can be expressed as a predominately soluble protein in the absence of DFF45. It is possible to reconcile these observations by considering the observation from BIAcore experiments that D2 has much slower kinetics of dissociation from and association with DFF40 in comparison to D1. It is reasonable to assume that the rapid kinetics of D1 allows it binds to nascent DFF40. Such initial interaction may thus be critical for the subsequent slow binding of D2 during the rapid translation phase, keeping DFF40 in the pathway towards maturation. Interestingly, we found the elements of DFF40 responsible for insolubility to map to the region coinciding with D2 binding. These observations lead to the conclusion that binding of D2 domain to DFF40, thus preventing aggregation, is the main component to DFF45's function as a chaperone for DFF40. As stable binding of D2 requires covalent linkage to either D1 or D3, solubilization of DFF40 is concomitant with stable repression.

ACKNOWLEDGMENTS

We are grateful to Yee-Joo Tan for help with BIAcore instrumentation. We also thank Drs. Wanjin Hong, Alan Porter, and Victor Yu for critical comments on the manuscript. P.L. is supported by a research fund from the National Science and Technology Board of Singapore.

REFERENCES

1. Wyllie, A. H., Kerr, J. F., and Currie, A. R. (1980) *Int. Rev. Cyto.* **68,** 251–306.
2. Enari, M., Sakahira, H., Okawa, O., Iwamatsu, A., and Nagata, S. (1998) *Nature* **391,** 43–50.
3. Liu, X., Zou, H., Slaughter, C., and Wang, X. (1997) *Cell* **89,** 175–184.
4. Sakahira, H., Enari, M., and Nagata, S. (1998) *Nature* **391,** 96–99.
5. Halenbeck, R., Macdonald, H., Roulston, A., Chen, T. T., Conroy, L., and Williams, L. T. (1998) *Curr. Biol.* **8,** 537–540.
6. Mukae, N., Enari, M., Sakahira, H., Fukuda, Y., Inazawa, J., Toh, H., and Nagata, S. (1998) **95,** 9123–9128.
7. Liu, X., Li, P., Widlak, P., Zou, H., Luo, X., Garrard, W. T., and Wang, X. (1998) *Proc. Natl. Acad. Sci. U.S.A.* **95,** 8461–8466.
8. McCarty, J. S., Toh, S. Y., and Li, P. (1999) Submitted.
9. Xie, Z., Schendel, S., Matsuyama, S., and Reed, J. C. (1998) *Biochem.* **37,** 6410–6418.
10. Jönsson, U., Fägerstam, L., Ivarsson, B., Johnsson, B., Karlsson, R., Alundh, K., Löfas, S., Persson, B., Roos, H., Rönnberg, I., Sjölander, S., Stenberg, E., Urbaniczky, C., Östlin, H., and Malmqvist, M. (1991) *Biotechniques* **11,** 620–627.
11. Inohara, N., Koseki, T., Chen, S., Wu, X., and Nunez, G. (1998a) *EMBO J.* **17,** 2526–2533.
12. Inohara, N., Koseki, T., Chen, S., Benedict, M. A., and Nunez, G. (1998b) *J. Biol. Chem.* **274,** 270–274.